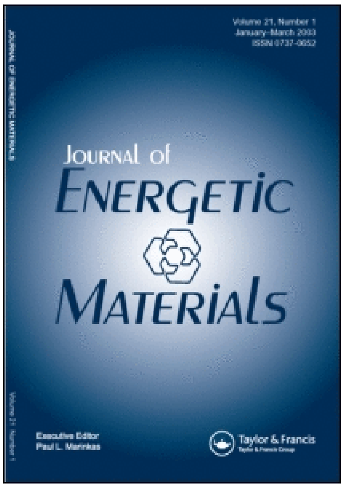

**Journal of Energetic Materials**
Publication details, including instructions for authors and subscription information:
http://www.informaworld.com/smpp/title~content=t713770432

# Theory and Modeling of Liquid Explosive Detonation

Craig M. Tarver[a]; Paul A. Urtiew[a]
[a] Energetic Materials Center, Lawrence Livermore National Laboratory, Livermore, California

**To cite this Article** Tarver, Craig M. and Urtiew, Paul A.(2010) 'Theory and Modeling of Liquid Explosive Detonation', Journal of Energetic Materials, 28: 4, 299 — 317
**To link to this Article: DOI:** 10.1080/07370651003789317
**URL:** http://dx.doi.org/10.1080/07370651003789317

*Journal of Energetic Materials*, 28: 299–317, 2010
Copyright © Taylor & Francis Group, LLC
ISSN: 0737-0652 print/1545-8822 online
DOI: 10.1080/07370651003789317

Taylor & Francis
Taylor & Francis Group

# Theory and Modeling of Liquid Explosive Detonation

CRAIG M. TARVER and
PAUL A. URTIEW

Energetic Materials Center, Lawrence Livermore
National Laboratory, Livermore, California

*The current understanding of the detonation reaction zones of liquid explosives is discussed in this article. The physical and chemical processes that precede and follow exothermic chemical reaction within the detonation reaction zone are discussed within the framework of the nonequilibrium Zeldovich-von Neumann-Doring (NEZND) theory of self-sustaining detonation. Nonequilibrium chemical and physical processes cause finite time duration induction zones before exothermic chemical energy release occurs. This separation between the leading shock wave front and the chemical energy release needed to sustain it results in shock wave amplification and the subsequent formation of complex three-dimensional cellular structures in all liquid detonation waves. To develop a practical Zeldovich-von Neumann-Doring (ZND) reactive flow model for liquid detonation, experimental data on reaction zone structure, confined failure diameter, unconfined failure diameter, and failure wave velocity in the Dremin-Trofimov test for detonating nitromethane are calculated using the ignition and growth reactive flow model.*

**Keywords:** detonation, ignition and growth, nitromethane

Address correspondence to Craig M. Tarver, Energetic Materials Center, Lawrence Livermore National Laboratory L-282, P.O. Box 808, Livermore, CA 94550-9234. E-mail: tarver1@llnl.gov

## Introduction

Dr. Anatoly Dremin was among the world leaders in energetic materials research for almost 50 years. Some of his extensive research is summarized in two excellent books [1,2]. He continued to contribute new ideas until his recent death [3–5]. Two of the areas in which Dr. Dremin made numerous contributions are the shock initiation and detonation of liquid explosives. This article discusses our current theoretical and reactive flow computer modeling efforts on the detonation of liquid explosives. The nonequilibrium Zeldovich-von Neumann-Doring (NEZND) theory was developed to identify the nonequilibrium chemical processes that precede and follow exothermic chemical energy release within the reaction zones of self-sustaining detonation waves in gaseous, liquid, and solid explosives [6–16]. Prior to the development of the NEZND model, the chemical energy released was merely treated as a heat of reaction in the conservation of energy equation in the Chapman-Jouguet (C-J) [17,18], Zeldovich-von Neumann-Doring (ZND) [19–21], and curved detonation wave front theories [22]. NEZND theory is consistent with many experimentally determined detonation wave properties that the ZND model cannot explain. These include induction time delays for the onset of chemical reaction; rapid rates of the chain reactions that form the reaction product molecules; de-excitation rates of the initially highly vibrationally excited products; the feedback mechanism that allows the chemical energy to sustain the leading shock wave front at an overall constant detonation velocity; and the establishment of the complex three-dimensional Mach stem shock front structure. Figure 1 illustrates the various processes that occur behind the 3D shock front in the NEZND model of detonation in condensed-phase explosives containing carbon, hydrogen, oxygen, and nitrogen atoms ($C_wH_xO_yN_z$). The detonation wave travels from left to right in Fig. 1. The chemical energy feedback mechanism is the amplification of pressure wavelets by excess vibrational energy initially present in excited reaction product molecules ($CO_2$, $CO$, $N_2$, $H_2O$, etc.) as the wavelets propagate through the reaction zone and overtake the shock front.

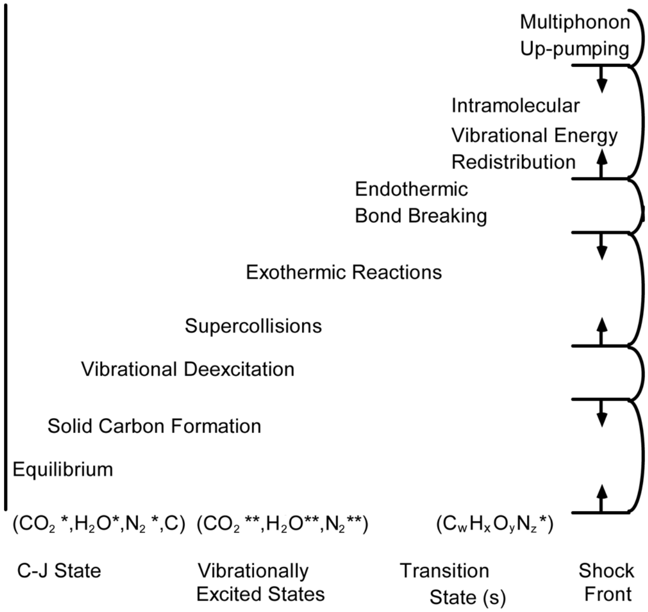

**Figure 1.** The nonequilibrium Zeldovich-von Neumann-Doring (NEZND) model of self-sustaining detonation in condensed-phase explosives.

It has been postulated by Dremin [2] and others that, in some very energetic homogeneous explosives, the chemical energy release occurs instantaneously during shock compression and thus the detonation wave fronts are stable; that is, they do not have a three-dimensional cellular structure. The next section of this article presents theoretical arguments and experimental data supporting the existence of finite duration induction time delays for exothermic chemical energy release in all liquid explosive detonation waves. Thus, these detonation waves are unstable and have cellular structures. The third section of this article presents the results of ignition and growth reactive flow modeling of the experimental data on the detonation reaction zone profile, confined failure diameter, unconfined failure diameter, and the Dremin-Trofimov failure wave velocity test for nitromethane. The final section presents the conclusions.

## The Onset of Exothermic Chemical Reaction in Liquid Detonation Waves

In condensed-phase detonation waves, the phonon modes are initially excited by the leading shock wave front, followed by multiphonon excitation of the lowest frequency vibrational modes called "doorway modes" [23] and then the higher frequency modes by multiphonon up-pumping and internal vibrational energy redistribution (IVR) [24]. Hong et al. [25] quantitatively measured these processes experimentally in shocked nitromethane using ultrafast infrared Raman spectroscopy. Many molecular dynamics studies, including those by Smirnov and Dremin [5], have shown that the rotational and vibrational temperatures are initially much lower than the translational temperatures behind shock waves, and it takes many collisions to establish complete thermal equilibration. All of the existing experimental and theoretical evidence supports the position that only after the explosive molecules have attained vibrational equilibrium can exothermic chemical decomposition begin [12]. Thus, at the high temperatures, densities, and pressures attained in the von Neumann state(s) of a liquid detonation wave, multiphonon up-pumping and IVR control the induction times for initial bond breaking reactions that are longer than those predicted by classical Arrhenius kinetics.

The induction time(s) for the initial thermal explosion behind the leading shock wave front(s) of a detonation wave can be calculated using the high-pressure, high-temperature transition state theory. Experimental unimolecular gas-phase reaction rates under low-temperature ($<1000\,\mathrm{K}$) shock conditions obey the classical Arrhenius reaction rate law:

$$K = A\ e^{-E/RT} \tag{1}$$

where $K$ is the reaction rate constant, $A$ is a frequency factor, $E$ is the activation energy, and $T$ is temperature. At higher temperatures, the measured rates are slower than predicted by Eq. (1). This phenomenon is called *falloff* [26]. In a statistical mechanics derivation called *starvation kinetics*, Eyring [27] attributed this falloff in unimolecular rates at the extreme temperature and density states attained in condensed-phase shock and detonation waves to the close proximity of vibrational states. This causes the high-frequency mode that becomes the transition state to rapidly equilibrate with the surrounding modes by IVR. These modes form a ‘‘pool’’ of vibrational energy in which the energy required for decomposition is shared. Any large quantity of vibrational energy that a specific mode receives from an excitation process is rapidly shared among the modes before reaction can occur. Conversely, sufficient vibrational energy from the entire pool of oscillators is statistically present in the transition state long enough to cause a reaction. When the total energy in the vibrational modes equals the activation energy, the reaction rate constant $K$ is

$$K = (kT/h)e^{-s}\sum_{i=0}^{s-1}(E/RT)^{i}e^{-E/RT}/i! \qquad (2)$$

where $k$, $h$, and $R$ are Boltzmann's, Planck's, and the gas constant, respectively, and $s$ is the number of neighboring vibrational modes equilibrating with the transition state. The main effects of rapid IVR among $s+1$ modes at high densities and temperatures are to decrease the rate constant dependence on temperature and to cause longer induction times at high temperatures.

The concept of starvation kinetics appears to be a general one that can explain the falloff in unimolecular decomposition rates at high temperature. The deviation from the reaction rate in Eq. (1) starts at approximately 1000 K in large molecules where $s$ approaches 20 and at approximately 3000 K in small molecules where $s$ is only 3 or 4. Reasonable reaction rate constants were calculated for several detonating solids and liquids using Eq. (2) with realistic equations of state and values of $s$ [12,14]. Nanosecond reaction zone measurements for solid explosives overdriven to pressures and temperatures exceeding those attained in self-sustaining detonation waves have shown that reaction rates increase very slowly with shock temperature [28].

For nitromethane, there are 15 vibrational modes, so $s = 14$. Reaction rate constants calculated using Eqs. (1) and (2) are now compared to induction time results for liquid nitromethane in Fig. 2 for various unreacted nitromethane equations of state. The average unreacted von Neumann spike state for nitromethane calculated using the CHEETAH chemical equilibrium code [29] based on an exponential six potential is 1575 K, and thus $1/T = 6.35 \times 10^{-3}\,\mathrm{K}^{-1}$. This von Neumann spike temperature agrees well with those calculated using the two analytical equations of state shown in Fig. 2. The highest unreacted temperatures and pressures are in the Mach stem portions of the three-dimensional shock wave front, where the shock velocities are estimated to be 1.1 times C-J detonation velocity [9]. The estimated maximum unreacted Mach stem shock temperatures for nitromethane are in the 2000–2500 K range [9], implying inverse temperatures of 4 to $5 \times 10^{-4}\,\mathrm{K}^{-1}$.

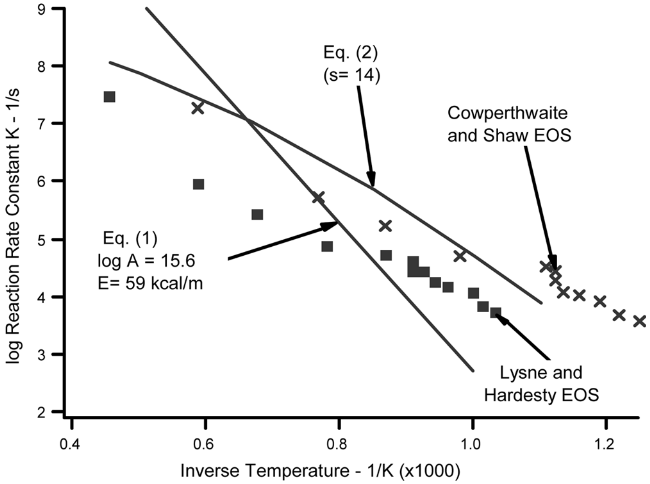

**Figure 2.** Reaction rate constant versus inverse temperature plots for shocked nitromethane.

These inverse temperatures predict picosecond (log $K = 12$) induction times based on Eq. (1). The nanosecond induction times predicted by Eq. (2) (log $K = 9$) have been observed experimentally for many explosives.

Experimental measurements of the reaction zone profiles of detonating nitromethane using nanosecond time-resolved VISAR laser interferometry have been reported by Sheffield et al. [30]. Two experimental reaction zone profiles are shown in Fig. 3. One record, taken with an older VISAR system, showed an induction time for exothermic reaction of 3 to 4 ns, whereas the profile taken by a newer VISAR system did not exhibit an induction time. Both profiles did show rapid decreases in particle velocity for about 10 ns, followed by slower decreases in particle velocity for another 40 to 50 ns. Nitromethane diluted with acetone has long been known [2,31,32] to exhibit unstable detonation with a measurable cellular structure. Dremin [2, comments in 30] argued that pure nitromethane also has an unstable front with a cellular structure. This cellular structure is extremely small and has not yet been directly observed.

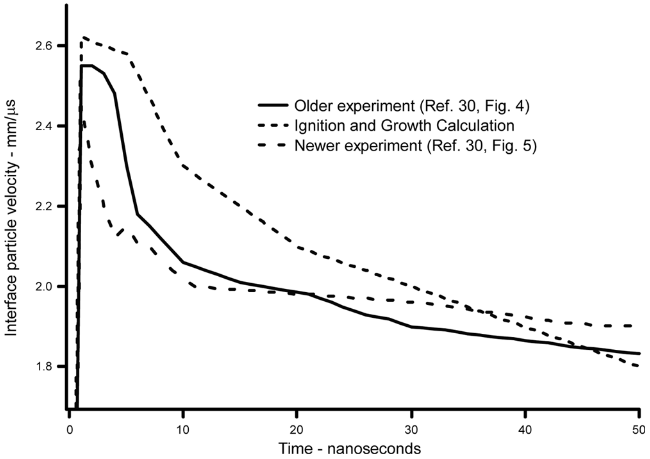

**Figure 3.** Interface particle velocity for detonating nitromethane and a PMMA window.

More energetic liquid explosives, such as nitroglycerine, have lower activation energy barriers than nitromethane, and their detonation wave cellular structures have not yet been resolved experimentally. The physical and chemical processes described above limit the rates of the initial bond breaking reactions and cause finite induction times. This will cause the formation of a cellular structure. Subnanosecond time-resolved experiments may eventually answer the question of the existence of stable liquid detonation waves [2].

## Ignition and Growth Model for Detonating Nitromethane

To estimate shock sensitivity and detonation performance characteristics of a liquid explosive in various geometries, a practical hydrodynamic computer code reactive flow model is needed. Homogeneous liquid and perfect crystal solid explosives contain no voids, which form hot spot reaction sites during shock compression and thus obey temperature-dependent reaction rate laws. Due to the uncertainty in the unreacted equation of state (see Fig. 2), it is not yet possible to accurately calculate the average von Neumann spike temperature. Thus, it is not possible to correctly calculate temperature based reaction rates under detonation conditions. As previously mentioned, the use of Eq. (1) predicts picosecond reaction rates that are too fast, and Eq. (2) is not currently available in most hydrodynamic codes. However, phenomenological reactive flow models based on the average one-dimensional ZND structure can be used to accurately predict two-dimensional effects, such as failure diameter. The ignition and growth model of shock initiation and detonation [33–39] has been applied to many shock initiation and detonation studies of solid explosives and propellants in many 1D, 2D, and 3D codes. To allow practical estimations of several liquid explosive detonation properties, a set of ignition and growth parameters for detonating nitromethane is developed in this section. The model uses two Jones-Wilkins-Lee (JWL) equations of state, one for the unreacted explosive and one for its reaction products, in the temperature dependent form:

$$p = Ae^{-R_1 V} - Be^{-R_2 V} + \omega\ C_v\ T/V \tag{3}$$

where $p$ is pressure in megabars, $V$ is relative volume, $T$ is temperature, $w$ is the Gruneisen coefficient, $C_v$ is the average heat capacity, and $A$, $B$, $R_1$, and $R_2$ are constants. The reaction rate law for the conversion of explosive to products is:

$$dF/dt = I(1-F)^b(\rho/\rho_0 - 1 - a)^x + G_1(1-F)^c F^d p^y + G_2(1-F)^e F^g p \tag{4}$$

$$0 < F < F_{\mathrm{igmax}}\ 0 < F < F_{\mathrm{G1max}}\ F_{\mathrm{G2min}} < F < 1$$

where $F$ is the fraction reacted, $t$ is time, $\rho$ is the current density, $\rho_0$ is the initial density, and $I$, $G_1$, $G_2$, $a$, $b$, $c$, $d$, $e$, $g$, $x$, $y$, and $z$ are constants. The mixture equations assume pressure and temperature equilibration between the unreacted explosive and its reaction products.

The unreacted JWL for nitromethane is fit to experimental shock compression data and the universal liquid Hugoniot equation of state [40]. The reaction product JWL equation of state is fit to the wall velocity expansion data from copper cylinder detonation tests [41]. The three-term rate law describes the three stages of reaction generally observed in shock initiation and detonation of heterogeneous solid explosives. For liquid explosive detonation modeling, the first term of Eq. (4) represents the ignition of the explosive as it is compressed by the leading 3D shock wave, creating hot regions at the triple shock interactions. The fraction of explosive ignited is set equal to 1% in less than a nanosecond. The second reaction rate in Eq. (4) models the rapid formation of the major reaction product gases ($CO_2$, $N_2$, $H_2O$, CO, etc.) in highly vibrationally excited states and their subsequent expansion and equilibration. Experimentally, this process has been measured to take approximately 10 ns [42]. The use of a high exponent on the pressure (4 in this case) in the second rate term of Eq. (4) simulates this rapid chemical energy release much like a temperature-based rate would. The third term in Eq. (4) is used to describe the relatively slow diffusion-controlled formation of nanometer-size solid carbon particles (diamond, graphite, or amorphous carbon) from single carbon atoms. For nitromethane, the last 20% of the chemical energy release is assumed to be due to solid graphite from smaller carbon species formation in a diffusion controlled process. Experimentally, the carbon formation has been observed to take approximately 50–60 ns [43]. A linear pressure-dependent rate in the third term of Eq. (4) simulates a diffusion-controlled reaction. Table 1 lists the equation of state and reaction rate parameters used in the ignition and growth nitromethane detonation model.

The experimental data on detonating nitromethane to which the ignition and growth model is applied include reaction zone particle velocity versus time VISAR measurements [30]; failure diameter in brass confinement [44]; unconfined (actually weakly confined) failure diameter [45]; and the Dremin-Trofimov failure wave velocity measurement made as a detonation wave propagates from a confined geometry into an unconfined geometry [46]. Figure 3 shows two experimental VISAR interface particle velocity histories for detonating nitromethane and poly(methyl methacrylate) (PMMA) windows measured by Sheffield et al. [30] and the ignition and growth calculated interface velocity. The calculated peak velocity, the duration of the induction time (∼1–4 ns), the time duration of a fast reaction (from ∼6 to 10 ns), and the time duration of a slow reaction (∼40 additional ns) agree with experiment to within 5%. The ignition and growth nitromethane parameters are used to calculate the other three sets of experimental data. Campbell and Engelke [44] reported a failure diameter of $2.84 \pm 0.42$ mm for nitromethane confined by 3.18-mm-thick brass walls. Ignition and growth calculations of this exact geometry produced a failure of detonation at 2.4 mm diameter and sustained detonation at 3.2 mm diameter. Campbell et al. [45] measured a failure diameter of 18 mm in weak (glass) confinement

**Table 1**
Ignition and growth parameters for nitromethane

| Initial density $r_0 = 1.137\,\text{g/cm}^3$ | | |
|---|---|---|
| Unreacted JWL | Product JWL | Reaction rates |
| $A = 30\,\text{Mbar}$ | $A = 2.092\,\text{Mbar}$ | $I = 1000\,\text{ms}^{-1}$ |
| $B = -0.018003\,\text{Mbar}$ | $B = 0.05689\,\text{Mbar}$ | $F_{\text{igmax}} = 0.01$ |
| $R_1 = 10$ | $R_1 = 4.4$ | $a = 0.5741$ |
| $R_2 = 1$ | $R_2 = 1.2$ | $b = 0.667$ |
| $w = 1.237$ | $w = 0.3$ | $x = 4$ |
| $Cv = 1.4272 \times 10^{-5}\,\text{Mbar/K}$ | $Cv = 1 \times 10^{-5}\,\text{Mbar/K}$ | $G_1 = 121{,}875\,\text{Mb}^{-4}\,\text{ms}^{-1}$ |
| $T_0 = 298\,\text{K}$ | $E_0 = 0.051\,\text{Mbar-cc/cc-g}$ | $F_{\text{G1max}} = 0.8$ |
| | | $c = 0.667$ |
| | | $d = 0.667$ |
| | | $y = 4$ |
| | | $G_2 = 240\,\text{Mb}^{-1}\,\text{ms}^{-1}$ |
| | | $F_{\text{G2min}} = 0.8$ |
| | | $e = 0.667$ |
| | | $g = 0.667$ |
| | | $z = 1.0$ |

and reported that other weak confining materials, such as cardboard, have yielded similar results. Thus, the weakly confined failure diameter of nitromethane is estimated to be between 18 and 20 mm [47]. Ignition and growth calculations of weakly confined nitromethane predicted failure to sustain detonation at 15 mm diameter and self-sustaining detonation at 20 mm diameter. Thus, the ignition and growth parameters based on the one-dimensional VISAR experimental data did produce heavily and weakly confined failure diameter estimations to within 10%.

One of the most important contributions to the understanding of how liquid explosives can exhibit very short reaction lengths, almost no detonation wave front curvatures, small velocity decreases before failure, and yet relatively large weakly confined failure diameters [2] is the failure wave measurement test of Dremin and Trofimov [46]. Enig and Petrone [48] provided an English translation and a detailed mathematical interpretation of the test. A heavily confined liquid explosive of a certain diameter greater than the confined failure diameter is detonated. After a long enough run distance to insure self-sustaining detonation, the detonation wave proceeds into a much larger diameter volume of the same liquid that is essentially unconfined. If the confined diameter of a liquid is less than the unconfined failure diameter, the detonation wave fails upon reaching the larger diameter. The rate of detonation wave failure can be measured by a streak camera as the absence of bright light in the ‘‘failure or dark wave’’ that propagates from the edge of the end of the confinement toward the center of the unconfined region. If the confined diameter is larger than the unconfined failure diameter, the detonation wave begins to fail upon entering the unconfined liquid, but reinitiation of detonation occurs in the shocked nitromethane behind the expanding unreacted shock wave before the detonation is totally extinguished. The two-dimensional analytical model [46,48] allows the states in the flow region to be calculated based on measured detonation and failure wave velocities. The physical mechanism of liquid detonation failure was found by Urtiew [49] to be the absence of the triple point interactions needed to sustain detonation at the outer edge of the cellular structure as the detonation enters the unconfined liquid.

Measured failure wave velocities for nitromethane were reported to be 4.75 mm/ms by Dremin and Tofimov [46] in axisymmetric geometry and 3.72 mm/ms by Davis in planar geometry (reported in Enig and Petrone [48]). In a detonation study of four liquid explosives that showed that the failure wave velocity increases with decreasing shock insensitivity of the liquid, Tarver et al. [47] measured a failure wave velocity of 3.88 mm/ms for nitromethane in cylindrical geometry. Though it cannot model the cellular structure of liquid detonation waves, the ignition and growth reactive flow model does correctly predict the average reaction rates measured in detonating nitromethane. Two-dimensional axisymmetric ignition and growth calculations of the Dremin-Trofimov test were performed for 10-, 15-, and 20-mm-diameter detonating nitromethane cylinders confined by lead [47] into unconfined nitromethane. The 10-mm-diameter charge failed completely, with a failure velocity very close to 4 mm/ms. The 15-mm-diameter calculation barely reinitiated near the center of the charge before the arrival of the failure wave in an unsteady manner that persisted for a long distance. The 20-mm-diameter calculation showed prompt reinitiation of steady detonation after a short distance of failure wave propagation. Therefore, the calculated unconfined failure diameter and failure wave velocity in the Dremin-Trofimov failure wave test agree closely with experimental data.

## Conclusions

The NEZND model was formulated to identify the nonequilibrium chemical and physical mechanisms that precede and follow the chemical energy release in self-sustaining detonation waves. In terms of homogeneous liquid explosives whose reaction rates obey Arrhenius kinetics, the processes of multiphonon up-pumping and IVR require many collisions before the vibrational, rotational, and translational energies are equilibrated behind a shock front. At high temperatures and densities behind the leading shock front of a liquid detonation wave, statistical pooling of vibrational energy with the neighboring vibrations causes even longer induction times for the initial unimolecular decomposition reaction. Induction time calculations using starvation kinetics yield good agreement with experimental data in the falloff temperature regime for nitromethane and many other unimolecular rates. More shock-sensitive liquids, such as nitroglycerine, have low energy barriers to unimolecular decomposition that still must be exceeded by the vibrational energy present in the transition state. This implies that finite induction times exist for chemical reaction in all liquid detonation waves. If the chemical energy release occurs at a finite distance behind the leading shock front, it amplifies pressure wavelets in the reaction zone. These pressure wavelets overtake the shock front and maintain its strength. With pressure wavelets arriving at various times, the leading shock cannot be one-dimensional and develops a complex three-dimensional cellular structure. This implies that three-dimensional cellular structures develop in all liquid detonation waves [50]. Subnanosecond time-resolved experiments are required to verify the existence of cellular structures for very sensitive liquids.

Hydrodynamic computer code predictions of liquid detonation wave properties in one-, two-, and three-dimensional geometries require a practical reactive flow model. The ZND theory-based ignition and growth model was applied to experimental detonation data on nitromethane with good results. Eventually, it will be possible to construct all Arrhenius temperature-dependent, multistep chemical decomposition reactive flow models that calculate cellular structures. The nitromethane model developed in this article can be used for safety and performance assessments. Similar parameter sets can be developed for other liquid explosives.

## Acknowledgments

The authors gratefully acknowledge many fascinating discussions with the late Dr. Anatoly Dremin. His obituary describes many facets of his life and scientific career [51]. This work was performed under the auspices of the United States Department of Energy by the Lawrence Livermore National Laboratory under Contract DE-AC52-07NA27344.

## References

[1] Dremin, A. N., S. D. Savrov, V. S. Trifimov, and K. K. Shvedov. 1970. *Detonation Waves in Condensed Media*. Moscow: Izd-vo Nauka.

[2] Dremin, A. N. 1999. *Toward Detonation Theory*. New York: Springer-Verlag.

[3] Dremin, A. N. 2008. Two-dimensional cellular structure of a kinetically unstable detonation front. *Combustion, Explosion and Shock Waves*, 44: 444–450.

[4] Dremin, A. N. 2006. On the limit of detonation on concentration of liquid explosive mixtures with nonexplosive diluents. *Thirteenth International Detonation Symposium*, pp. 720–725, July 23–28. Norfolk, VA.

[5] Smirnov, A. L. and A. N. Dremin. 2006. Molecular dynamics modeling of shock and detonation phenomena in liquids of polyatomic molecules. *Thirteenth International Detonation Symposium*, pp. 1241–1246, July 23–28. Norfolk, VA.

[6] Tarver, C. M. 1973. *On the Chemical Energy Release in Self-Sustaining Detonation Waves in Gaseous and Condensed Explosives*. Ph.D. thesis, The Johns Hopkins University: Baltimore, MD.

[7] Tarver, C. M. 1982. Chemical energy release in one-dimensional detonation waves in gaseous explosives. *Combustion and Flame*, 46: 111–133.

[8] Tarver, C. M. 1982. Chemical energy release in the cellular structure of gaseous detonation waves. *Combustion and Flame*, 46: 135–156.

[9] Tarver, C. M. 1982. Chemical energy release in self-sustaining detonation waves in condensed explosives. *Combustion and Flame*, 46: 157–176.

[10] Tarver, C. M., L. E. Fried, A. J. Ruggerio, and D. F. Calef. 1993. Energy transfer in solid explosives. *Tenth International Detonation Symposium*, pp. 3–10, July 12–16. Boston, MA.

[11] Tarver, C. M. 1997. Chemical reaction and equilibration mechanisms in detonation waves. In S. C. Schmidt, D. P. Dandekar, and

J. W. Forbes (eds.), *Shock Compression of Condensed Matter–1997*, pp. 301–304. New York: AIP Press.

[12] Tarver, C. M. 1997. Multiple roles of highly vibrationally excited molecules in the reaction zones of detonation waves. *Journal of Physical Chemistry A*, 101: 4845–4851.

[13] Tarver, C. M. 1999. Next generation experiments and models for shock initiation and detonation of solid explosives. In M. D. Furnish, L. C. Chhabildas, and R. S. Hixan (eds.), *Shock Compression of Condensed Matter–1999*, pp. 883–887. New York: AIP Press.

[14] Tarver, C. M. 2001. What is a shock wave to an explosive molecule? In M. D. Furnish, N. N. Thadhani, and Y. Horie (eds.), *Shock Compression of Condensed Matter–2001*, pp. 42–49. New York: AIP Press.

[15] Tarver, C. M. 2003. What is a shock wave to an explosive molecule? In Y. Horie, L. Davison, and N. N. Thadhani (eds.), *High-Pressure Shock Compression VI: Old Paradigms and New Challenges*, pp. 323–340. New York: Springer-Verlag.

[16] Tarver, C. M. 2005. Amplification of pressure waves during vibrational equilibration of excited chemical reaction products. *Russian Journal of Chemical Physics*, 4: 31–38.

[17] Chapman, D. L. 1899. Detonation Waves. *Philosophical Magazine 213, Series 5*, 47: 90–104.

[18] Jouguet, E. J. 1904. Theory of Detonation, Parts 1 & 2. *Journal of Pure and Applied Mathematics 70, Series 6*, 1: 347; 2:5.

[19] Zeldovich, Y. B. 1940. Theory of detonation. *Journal of Experimental and Theoretical Physics (USSR)*, 10: 542–568.

[20] Von Neumann, J. 1942. *Theory of Detonation Waves*. Washington, DC: Office of Science Research and Development. Report No. 549.

[21] Doring, W. 1943. Detonation waves. *Ann. Phys. 5e Folge*, 43: 421–436.

[22] Wood, W. W. and J. G. Kirkwood. 1958. Present status of detonation theory. *Journal of Chemical Physics*, 29: 957–958.

[23] Dlott, D. D. and M. D. Fayer. 1990. Shocked molecular solids: Vibrational up pumping, defect hot spot formation, and the onset of chemistry. *Journal of Chemical Physics*, 92: 3798–3812.

[24] Weston, R. E., Jr. and G. W. Flynn. 1993. Intramolecular vibrational energy transfer. *Annual Reviews of Physical Chemistry*, 43: 559–599.

[25] Hong, X., S. Chen, and D. D. Dlott. 1995. Ultrafast mode-specific intermolecular vibrational energy transfer to liquid nitromethane. *Journal of Physical Chemistry*, 99: 9102–9109.

[26] Kiefer, J. H., S. S. Kumaran, and S. Sundaram. 1993. Vibrational relaxation, dissociation, and dissociation incubation times in norborene. *Journal of Chemical Physics*, 99: 3531–3541.

[27] Eyring, H. 1978. Starvation kinetics. *Science*, 199: 740–743.

[28] Green, L. G., C. M. Tarver, and D. J. Erskine. 1989. Reaction zone structure in supracompressed detonating explosives. In *Ninth Symposium (International) on Detonation*, pp. 670–682, August 28–September 1. Portland, OR: Office of the Chief of Naval Research. OCNF 113291-7.

[29] Fried, L. E. and W. M. Howard. 2001. *Cheetah 3.0 Users Manual.* Livermore, CA: Lawrence Livermore National Laboratory. Report UCRL-MA-117541.

[30] Sheffield, S. A., R. Engelke, R. R. Alcon, R. L. Gustavsen, D. L. Robbins, D. B. Stahl, H. L. Stacy, and M. C. Whitehead. 2002. Particle velocity measurements of the reaction zone in nitromethane. In *Twelfth International Symposium on Detonation.* San Diego, CA: Office of Naval Research. ONR 333-05-2.

[31] Urtiew, P. A. and A. S. Kusubov. 1970. Wall traces of detonation in nitromethane-acetone mixtures. In *Fifth Symposium (International) Symposium on Detonation.* Pasadena, CA: Office of Naval Research. ACR-184.

[32] Fickett, W. and W. C. Davis. 1979. Detonation, Berekeley: University of California Press.

[33] Tarver, C. M., J. O. Hallquist, and L. M. Erickson. 1985. Modeling short pulse duration shock initiation of solid explosives. In *Eighth Symposium (International) on Detonation*, pp. 951–961, July 15–19. Albuquerque, NM: Naval Surface Weapons Center. NSWC MP 86-194.

[34] Tarver, C. M., J. W. Kury, and R. D. Breithaupt. 1997. Detonation waves in triaminotrinitrobenzene. *Journal of Applied Physics*, 82: 3771–3782.

[35] Kury, J. W., R. D. Breithaupt, and C. M. Tarver. 1999. Detonation waves in trinitrotoluene. *Shock Waves*, 9: 227–237.

[36] Tarver, C. M. 2005. Ignition and growth modeling of LX-17 hockey puck experiments. *Propellants, Explosives, Pyrotechnics*, 30: 109–117.

[37] Tarver, C. M. and E. M. McGuire. 2002. Reactive flow modeling of the interaction of TATB detonation waves with inert

materials. In *Twelfth International Symposium on Detonation*. San Diego, CA: Office of Naval Research. ONR 333-05-2.

[38] Garcia, M. L. and C. M. Tarver. 2006. Three-dimensional ignition and growth reactive flow modeling of prism failure tests on PBX 9502. In *Thirteenth International Detonation Symposium*, pp. 63–70, July 23–28. Norfolk, VA: Office of Naval Research. ONR 351-07-01.

[39] Tarver, C. M. and S. K. Chidester. 2007. Ignition and growth modeling of detonating TATB cones and arcs. In M. Elert, M. D. Furnish, R. Chau, N. C. Holmes, and J. Nguyen (eds.), *Shock Compression of Condensed Matter–2007*, pp. 429–432. Waikoloa, HI.

[40] Woolfolk, R. W., M. Cowperthwaite, and R. Shaw. 1973. A universal Hugoniot for liquids. *Thermochemica Acta*, 5: 409–414.

[41] Dobratz, B. M. and P. C. Crawford. 1985. *LLNL High Explosive Handbook*. Livermore, CA: Lawrence Livermore National Laboratory. Report UCRL-52997 Change 2.

[42] Craig, B. G. 1965. Measurements of the detonation front structure in condensed phase explosives. In *Tenth Symposium (International) on Combustion*, pp. 863–867. Pittsburgh, PA: The Combustion Institute.

[43] Petrone, F. J. 1968. Validity of the classical detonation wave structure for condensed explosives. *Physics of Fluids*, 11: 1473–1478.

[44] Campbell, A. W. and R. Engelke. 1976. The diameter effect in high density heterogeneous explosives. *Sixth Symposium (International) on Detonation*, pp. 642–652, August 24–27. Coronado, CA.

[45] Campbell, A. W., M. E. Malin, and T. E. Holland. 1956. Temperature effects in the liquid explosive nitromethane. *Journal of Applied Physics*, 27: 963.

[46] Dremin, A. N. and V. S. Trofimov. 1965. On the nature of the critical diameter. In *Tenth Symposium (International) on Combustion*, pp. 839–843. Pittsburgh, PA: The Combustion Institute.

[47] Tarver, C. M., R. Shaw, and M. Cowperthwaite. 1976. Detonation failure diameter studies of four liquid nitroalkanes. *Journal of Chemical Physics*, 64: 2665–2673.

[48] Enig, J. W. and F. J. Petrone. 1970. The failure diameter theory of Dremin. In *Fifth Symposium (International) Symposium on Detonation*, pp. 99–104, August 18–21. Pasadena, CA: Office of Naval Research. ACR-184.

[49] Urtiew, P. A. 1975. From cellular structure to failure waves in liquid detonations. *Combustion and Flame*, 25: 241–245.

[50] Fickett, W. and W. C. Davis. 1979. *Detonation Theory and Experiment*, Mineola, NY: Dover Publications.

[51] Deribas, A., R. M. Doherty, C.-O. Leiber, and S. Zeman. 2008. Obituary Anatoly N. Dremin 1930–2008. *Propellants, Explosives, Pyrotechnics*, 33: 85–86.